DOI: 10.26599/FSHW.2026.9251021

Contents lists available at SciOpen

Food Science and Human Wellness

journal homepage: https://www.sciopen.com/journal/2097-0765

China Food Publishing Co.

A Lactoferrin-Based Formulation Ameliorates Immune Dysfunction and Improves Growth in a Rat Model of Marginal Zinc Deficiency

Zifu Zhao[#abc], Ignatius Man-Yau Szeto[#cde], Qi Xin[ab], Xuemin Wang[cde], Ruonan Wang[ab], Sufang Duan[cde], Libo Liu[ab], Guofang Zhang[ab], Chun Li*[a], Jian He*[cde]

[a.] *Key Laboratory of Dairy Science, Ministry of Education, College of Food Science, Northeast Agricultural University, Harbin 150030, China*

[b.] *Heilongjiang Green Food Science Research Institute, National Dairy Engineering Technology Research Center, Harbin 150028, China*

[c.] *Inner Mongolia Yili Industrial Group Co., Ltd., Hohhot, Inner Mongolia, 010110, China*

[d.] *Inner Mongolia Dairy Technology Research Institute Co., Ltd., Hohhot, Inner Mongolia, 010110, China*

[e.] *National Center for Technology Innovation of Dairy, Ltd., Hohhot, Inner Mongolia, 010110, China*

ABSTRACT: Marginal zinc deficiency (MZD) affects immunity, growth, and development in children. Therefore, effective interventions using food-derived functional components to enhance immunity are required. Although the immunomodulatory effects of bioactives, such as LF, colostrum, and yeast β-glycan have been previously established, their combined effects on MZD is unknown. Therefore, the systemic regulatory effects of a lactoferrin-based MZD formulation were investigated in this study. To establish a MZD model, weaned Sprague–Dawley rats were fed a diet containing 10 mg/kg zinc for 5 weeks. The rats were administered a lactoferrin-based formulation via oral gavage. Compared with the control group, zinc deficiency significantly affected body weight gain, femur development, organ index, NK cell activity, splenic lymphocyte proliferation, and cytokine levels. These indicators significantly improved after the lactoferrin-based formulation intervention. The high-concentration lactoferrin formulation (LFC_high) group showed the most significant recovery compared with that of the other groups. The NK cell activity increased from 12.25% in the Model group to 34.50% in the LFC_high group, and splenic lymphocyte proliferation increased from 9.30% in the Model group to 17.31% in the LFC_high group. Furthermore, the lactoferrin-based formulation effectively regulated the gut microbiota, increasing the abundance of beneficial bacteria and decreasing the relative abundance of harmful bacteria. These preclinical findings provide a foundation for exploring interventions to address MZD and future research on targeted nutritional strategies.

Keywords: Marginal zinc deficiency, Immune regulation, Lactoferrin, Gut microbiota, Zinc

1. Introduction

Zinc, an essential trace element, plays a major role in maintaining life through immune system, growth, reproductive health, and cognitive functions[1]. The precise assessment of the nutritional status of zinc is crucial because of its pleiotropic effects. The International Zinc Nutrition Consultative Group (IZiNCG) developed a "composite index of risk of zinc deficiency" using food consumption and child growth data to assess zinc status across populations[2]. This index defines high-risk populations as those with ≥25% of individuals consuming less than the

[#]These authors contributed equally to this work
***Corresponding author**
Chun Li, spxylch@126.com; Jian He, warmstar0224@126.com

Received 8 December 2025
Received in revised from 22 January 2026
Accepted 4 March 2026

estimated average requirement (EAR) and >20% of preschool children exhibiting stunting. Moderate risk was defined as 15–25% with inadequate zinc intake and 10–20% of preschool children exhibiting stunting[3]. A WHO 2022 report indicated a 31% global prevalence of zinc deficiency, including >60% of Chinese children aged 0–14 years (Chinese National Center for Food Safety Risk Assessment). IZiNCG assessments using the Chinese National Nutrition and Health Survey data revealed that approximately 35.60% of the population had zinc intake below the EAR, and only 46.52% met or exceeded the recommended nutrient intake[2], indicating that >20% of Chinese preschool children experience moderate or marginal zinc deficiency (MZD).

MZD presents is challenging due to its subtle, non-specific symptoms, which often overlap with other health issues[4]. However, a prolonged deficiency can significantly impair immune function and increase the risk of infection. This highlights the need for effective interventions using food-derived functional components to enhance immunity. Natural bioactives, such as yeast β-glucan[5-7], colostrum, and lactoferrin (LF), a key component of milk, have robust immunomodulatory effects. LF activates immune cell maturation, migration, antimicrobial activity, and gut development[8-10]. Colostrum is richer in immunoglobulins and growth factors than regular milk, promotes immune regulation, and improves gut health. Yeast β-glucan, a natural polysaccharide, activates macrophages and T lymphocytes, promotes cytokine secretion, and boosts antioxidant activity[12-13]. These components specifically target MZD-related immune dysfunctions and provide targeted support to at-risk individuals.

The immunomodulatory effects of LF, colostrum, and yeast β-glucan are well established; however, research on their combined effects in alleviating MZD-induced immunodeficiency is limited and the dose-response relationship for LF remains unclear. Therefore, we investigated the effects of an LF-rich formulation in an MZD-induced immunodeficient rat model (a standard preclinical model for MZD research). We systematically evaluated the effects of the formulation on growth indicators, organ development, immune cell activity, proliferation or differentiation, and gut microbiota modulation to elucidate the regulatory mechanisms of MZD to provide a scientific basis for early identification and effective intervention of MZD, ultimately improving public health.

2. Materials and Methods

2.1 Materials

YAC-1 rat lymphoma cells were obtained from Beina Chuanglian Biotechnology Co. Ltd. Forty-eight 3-week old male Sprague–Dawley rats (60 ± 10 g) were purchased from Beijing Vital River Laboratory Animal Technology Co. Ltd. [Animal license: SCXK(Jing)2021-0006]. This study was approved by the Ethics Review Committee of the College of Food Science, Northeast Agricultural University (approval no. NEAUEC20240405). LF, colostrum, and yeast β-glucan were purchased from Inner Mongolia Yili Industrial Group Co. Ltd. The ELISA kits were obtained from Jiangsu Enzyme Immunoassay Industry Co. Ltd. Concanavalin A (Con A), MTT, dimethyl sulfoxide, and hematoxylin and eosin (HE) staining kits were purchased from Beijing Solarbio Science & Technology Co. Ltd. (Beijing, China). ACK lysis buffer, RPMI 1640 medium, fetal bovine serum, and phosphate-buffered saline (PBS) were purchased from Beijing Biosynthesis Biotechnology Co. Ltd. (Beijing, China). The rat regulatory T cell and rat Th17 staining kits were purchased from Hangzhou Lianke Biotechnology Co. Ltd. (Hangzhou, China).

2.2 Methods

2.2.1 Experimental grouping and intervention conditions

An MZD model was established according to the modified AIN-93G standard, as previously described, with some modifications (Table 1). The 48 rats were weaned at 3 weeks old and fed a standard diet for a 3-d acclimatization period. Subsequently, the animals were randomly divided into two main dietary regimens for a 5-week modeling period (Fig. 1): a zinc-deficient diet group (n=48) and a zinc-adequate control group (n=8).

Table 1 Feed Composition Ratio

Class	Ingredients	10ppm (Zn)	30ppm (Zn)
Carbohydrate	Sucrose, Fine Granulated	222.40	221.828
Mineral	Calcium Carbonate, Light, USP	357.00	357.00
Mineral	Potassium Phosphate, Monobasic	196.00	196.00
Mineral	Sodium Chloride	74.00	74.00
Mineral	Potassium Citrate, Monohydrate	70.78	70.78
Mineral	Potassium Sulfate	46.40	46.60
Mineral	Magnesium Oxide, Heavy, DC USP	24.00	24.00
Mineral	Ferric Citrate	6.06	6.06
Mineral	Zinc Carbonate	0.286	0.858
Mineral	Sodium Metasilicate	1.45	1.45
Mineral	Manganese Carbonate Hydrate	0.63	0.63
Mineral	Copper Carbonate	0.30	0.30
Mineral	Chromium Potassium Sulfate	0.28	0.28
Mineral	Boric Acid	0.08	0.08
Mineral	Sodium Fluoride	0.03	0.03
Mineral	Nickel (II) Carbonate	0.02	0.02
Mineral	Lithium Chloride, anhydrous	0.02	0.02
Mineral	Sodium Selenate	0.01	0.01
Mineral	Potassium Iodate	0.01	0.01
Mineral	Ammonium Molybdate Tetrahydrate	0.01	0.01
Mineral	Ammonium (meta)vanadate	0.01	0.01
Total		1000.00	1000.00

Control group	**Con**	Free consumption of feed containing 30 mg/kg of zinc
Model group	**Model**	Free consumption of low-zinc feed containing 10 mg/kg zinc
Treat group	**LF Treat**	**Model** + Gavage LF 50 mg/kg
	LFC_low	**Model** + Gavage of LF 10 mg/kg, and bovine colostrum 60 mg/kg, yeast β-glucan 9 mg/kg
	LFC_mid	**Model** + Gavage of LF 50 mg/kg, and bovine colostrum 60 mg/kg, yeast β-glucan 9 mg/kg
	LFC_high	**Model** + Gavage of LF 100 mg/kg, and bovine colostrum 60 mg/kg, yeast β-glucan 9 mg/kg

Fig. 1 Temperature: 22±2 ℃, Humidity: 50±10%, 12 h day-night cycle, four rats per cage. Feed time: All groups have a duration of 5 weeks. (LF, bovine colostrum, and yeast β-glucan were thoroughly mixed together in sterile distilled water to form a homogeneous suspension for oral gavage)

2.2.2 Body weight and immune organ index

The rats were conventionally housed for 35 d. General observations, including animal behavior, food and water intake, and defecation, were recorded daily. Body weight was measured weekly. At the end of the experiment, the animals were euthanized via intravenous anesthetic injection and blood was collected via cardiac puncture. The

thymus and spleen were immediately harvested and weighed, and thymus and spleen indices were calculated[14]. Samples were stored at -80 ℃ in sterile containers until further analysis. The thymus and spleen indices were calculated as follows:

$$\text{Thymus index}(\%) = \frac{\text{Thymus weight(g)}}{\text{Body weight(g)}} \times 100\% \quad \textit{Eq. (2.1)}$$

$$\text{Spleen index}(\%) = \frac{\text{Spleen weight(g)}}{\text{Body weight(g)}} \times 100\% \quad \textit{Eq. (2.2)}$$

2.2.3 NK cell activity

Target and effector cells (100 μL each, effector: target ratio 50:1) were added to 96-well plates, as previously described by Park[15]. Target cell spontaneous release wells contained 100 μL of target cells and medium, and maximum release wells contained 100 μL of target cells and 2.5% Triton X-100. All experiments were performed in triplicate. Plates were incubated at 37 °C with 5% CO_2 for 4 h. The supernatant (100 μL) from each well was transferred to a new 96-well plate, and 100 μL of lactate dehydrogenase (LDH) substrate solution was added. After a 3–10-min reaction, 30 μL of 1 M HCl was added to each well. The absorbance at 490 nm was measured using a microplate reader. The NK cell activity was calculated as follows:

$$\text{NK cell activity}(\%) = \frac{\text{OD Reaction well} - \text{OD Natural release well}}{\text{OD Maximum Release Hole} - \text{OD Natural release well}} \times 100\% \quad \textit{Eq. (2.3)}$$

2.2.4 Spleen lymphocyte proliferation capacity

Splenocyte proliferation was assessed using the MTT assay, as described by Wang[16]. Splenocyte suspensions were prepared using the harvested rat spleens and adjusted to 3,000–10, 000 cells per well using a hemocytometer. The adjusted suspension (100 μL) was added to each well of a 96-well plate (two wells per spleen sample). One well per sample received 7.5 μg/mL Con A (stimulated group), while the other served as an unstimulated control group. Triplicate wells were used for each group. Plates were incubated at 37 °C with 5% CO_2 for 72 h. At 68 h, supernatants were removed, and 90 μL of fresh medium and 10 μL of MTT solution (5 mg/mL) were added to each well. After a 4-h incubation, the supernatants were removed, and 110 μL of formazan solubilization solution was added to each well. The plates were gently shaken for 10 min to dissolve formazan crystals. The absorbance at 490 nm was measured using a microplate reader. Blank (medium, MTT, and formazan solution) and control (cells, medium, MTT, and formazan solution) wells were analyzed in triplicate for data normalization.

$$\text{Spleen Lymphocyte Proliferation}(\%) = (\text{OD test compound} - \text{OD con compound}) \times 100\% \quad \textit{Eq. (2.4)}$$

2.2.5 Staining of colon and thymus tissues

The spleens and colons were harvested, fixed in 4% paraformaldehyde, and embedded in paraffin. Sections (4 μm) were prepared using a cryostat. Colon sections were stained with HE and Alcian blue-periodic acid-Schiff (AB-PAS), whereas thymus sections were only stained with HE. The splenic and colonic morphologies were examined under a light microscope (Leica DM I8, Germany).

2.2.6 Detection of cytokines in serum and the colon

Following cardiac puncture, the serum was isolated by centrifuging the blood at 300 × *g* for 10 min. Serum IgA, IL-10, and IL-1β levels were determined using ELISA kits, according to the manufacturer's instructions. Frozen intestinal tissue samples were homogenized in ice-cold PBS (pH 7.4) and centrifuged at 300 × *g* for 10 min to obtain supernatants. Rat secretory IgA (sIgA) levels were determined using ELISA kits according to the manufacturer's instructions.

2.2.7 Flow cytometry of Th17 and Treg cells

Splenocytes were resuspended in RPMI 1640 complete medium at a concentration of 1×10^7 cells/mL. Cells were stained using a rat flow cytometry staining kit according to the manufacturer's instructions, and analyzed for Th17 and Treg cell populations using a FACSCelesta flow cytometer (BD Biosciences, USA).

2.2.8 Fecal intestinal flora analysis

Total genomic DNA was extracted from colonic contents using the cetyltrimethylammonium bromide method. The V3-V4 region of the *16S* rRNA gene was amplified using specific primers 341F (5'-CCTAYGGGRBGCASCAG-3') and 806R (5'-GGACTACNNGGGTATCTAAT-3'). The libraries were sequenced on an Illumina NovaSeq platform. Amplicon sequence variants were generated and those with an abundance <5 were filtered. Data sausing QIIME2 software (Novogene, Beijing, China).

2.2.9 Statistical analysis

Data were analyzed using SPSS version 26.0. Results are expressed as mean ± standard deviation ($n \geq 3$). One-way analysis of variance was used for statistical analysis, with $P < 0.05$ considered statistically significant.

3. Results

3.1 Ameliorative effects of the lactoferrin-based formulation on growth performance and femoral development in MZD rats

Significant differences in body weight were evident from 3 weeks after induced MZD, with the model group exhibiting a notable decrease compared with that of the control and all intervention groups (Fig. 2A,B). This trend persisted for 5 weeks. Concurrently, the gradual body weight gain induced by zinc deficiency was mitigated as the concentration of the interventions increased, with the most pronounced effect observed in the LFC_high group. Furthermore, alterations in feed utilization were key factors contributing to changes in body weight, with the control group demonstrating a gradual increase from an initial 13.72% to 22.93%, whereas the model group consistently exhibited higher feed utilization throughout the experimental cycle (Fig. 2C,D). This suggests that zinc deficiency is associated with relatively low feed utilization rates. In contrast, LFC_low exhibited a moderate increase in feed utilization, indicating a more stable feeding efficiency. Notably, LFC_mid and LFC_high reached the lowest point of feed utilization in the third week, after which it slightly increased but remained at an overall low level. Notably, LFC_high showed the lowest performance (19.67%) in the fifth week, demonstrating a significant increase in feeding efficiency ($P < 0.05$).

Moreover, a comparative analysis was conducted on the femoral weights and lengths of rats across various treatment groups. The Con group had a mean femoral weight of 1.36 g and length of 3.95 cm. The Model group had a significantly lower mean femoral weight (0.84 g), representing a 37.78% reduction in femoral weight. Additionally, the mean femoral length was reduced to 3.70 cm, indicating a 6.33% reduction (Fig. 2E,F). These results demonstrate that LF and its combination mitigated femoral dysplasia caused by zinc deficiency to a certain extent. Both femur length and weight demonstrated concomitant recovery with increasing LF concentrations, indicating a dose-dependent relationship. Notably, LFC_high, which exhibited a femur weight of 1.40 g and length of 3.875 cm (Fig. 2E,F), did not significantly differ from the control group ($P > 0.05$). This finding indicates that the combination of LF, yeast-β-glucan, and colostrum significantly promoted bone development in animals under zinc deficiency.

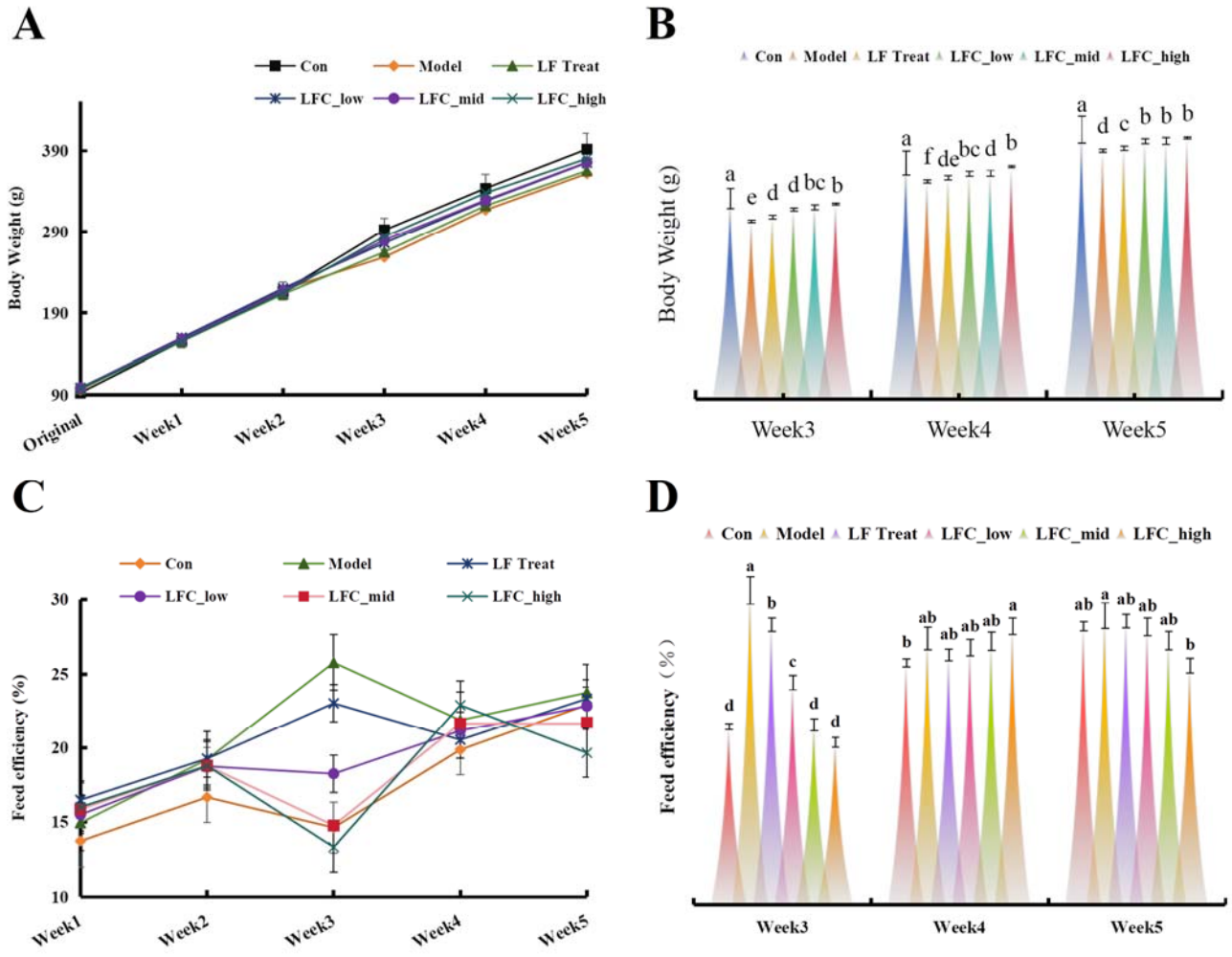

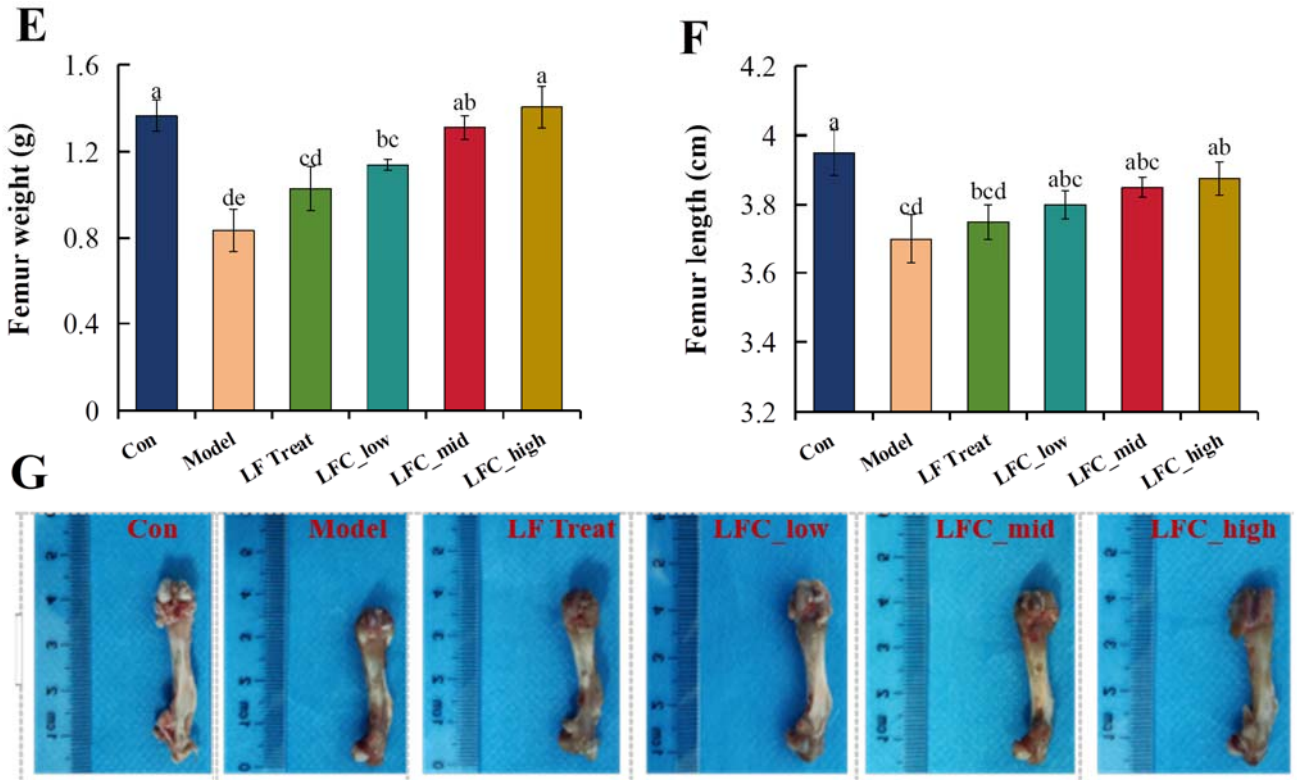

Fig. 2 Effects of the lactoferrin-based formulation on growth performance and femoral development in MZD rats.(A) Body weight gain over 5 weeks. (B) Weekly body weight at week 3-5.(C) Feed utilization efficiency over 5 weeks.(D) Weekly feed utilization efficiency at week 3-5. (E) Femoral weight at experiment end.(F) Femoral length at experiment end.(G) Representative femoral photographs Data are presented as mean ± SD (n=8).

3.2 Repairing effects of the lactoferrin-based formulation on immune organ indices and spleen morphology in MZD rats

The effect of zinc deficiency on thymus and spleen indices, and potential ameliorative effects of different concentrations of LF-based formulations were investigated. Compared with the Con group (Fig. 3A), the zinc-deficient Model group showed a significantly reduced thymus index (0.19, 22.33% decrease; $P < 0.05$). Intervention with the LF-based formulation resulted in thymus index recovery, with increased recovery observed at higher LF concentrations. The LFC_high group showed near-complete recovery, with a reduction of only 1.21% compared with that of the control group ($P > 0.05$). Similar trends were observed for the spleen index, indicating that the LF-based formulation alleviated the thymus and spleen hypoplasia induced by prolonged zinc deficiency (Fig. 3B). Moreover, HE staining of splenic sections from zinc-deficient rats revealed small splenocytes, disorganized cellular arrangement, increased intercellular space, and infiltration (Fig. 3C). LFC_mid and LFC_high groups showed improved splenocyte morphology, resulting in a dense cellular arrangement, reduced intercellular space and infiltration, and staining patterns closer to those of the control group.

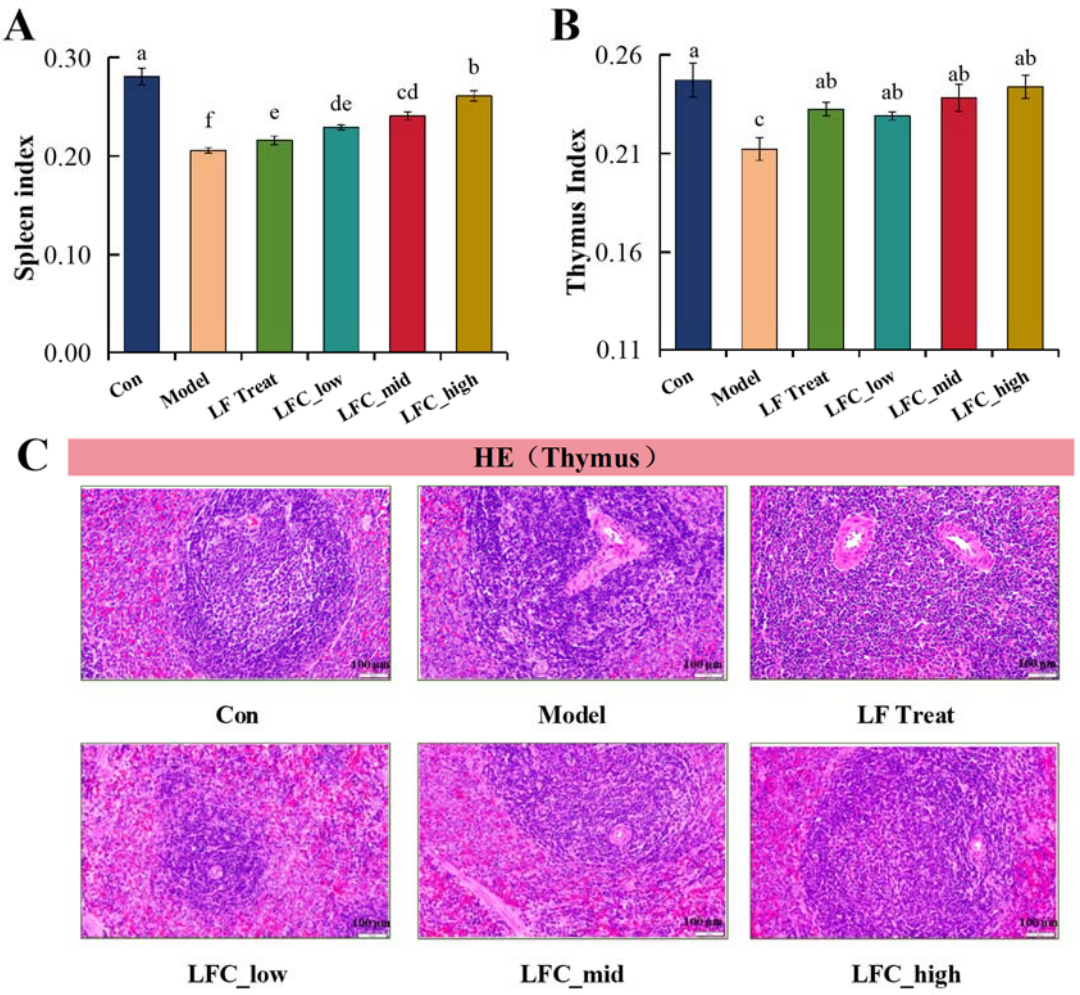

Fig. 3 Effects of zinc deficiency and the lactoferrin-based formulation on immune organ indices and spleen morphology. (A) Thymus index. (B) Spleen index. (C) Representative hematoxylin and eosin (H&E) stained sections of spleen tissue (scale bar = 100 μm). Data in A and B are presented as mean ± SD (n=8).

3.3 Regulatory effects of the lactoferrin-based formulation on the immune cell function and serum cytokine profile in MZD rats

We further investigated NK cell activity and splenocyte proliferation, which are key indicators of immune function (Fig. 4A,B). Compared with the control group, the Model group showed a significant 56.30% reduction in splenocyte proliferation ($P < 0.05$)[17]. Interventions using the LF-based formulation progressively alleviated this reduction. Specifically, compared with the control group, the LF Treat group showed a 51.23% reduction (11.10% increase compared to the model group), with greater recovery observed at higher LF concentrations ($P < 0.05$). The LFC_low, LFC_mid, and LFC_high groups showed reductions of 44.67%, 27.71%, and 18.80%, respectively, compared with 19.82%, 40.63%, and 51.61% reductions, respectively, in the Model group (Fig. 4B). Similarly, NK cell activity in the Model group was significantly reduced by 69.67% compared with that in the control group ($P < 0.05$). Intervention with the LF formulation resulted in recovery. The LF treatment group showed a 59.00% reduction (26.53% increase compared with the Model group), whereas the LFC_low, LFC_mid, and LFC_high groups showed reductions of 54.00%, 35.41%, and 14.37%, compared with 35.72%, 56.71%, and 71.30% increases, respectively, in the Model group (Fig. 4A).

Prolonged zinc deficiency significantly reduced the levels of all four cytokines ($P < 0.05$) compared with those in the control group. Intervention with the LF-based formulations resulted in varying degrees of recovery. Specifically, the model group showed a 13.40% reduction in IgA compared with that in the control group, but intervention with the LF formulation resulted in increases of 1.00% (LF Treat), 4.52% (LFC_low), 6.82% (LFC_mid), and 9.13% (LFC_high) relative to those of the Model group (Fig. 4C). Moreover, the Model group exhibited a 26.11% reduction in TNF-α compared with that in the control group. After the intervention, the LFC_low group exceeded control levels by 4.47% ($P > 0.05$), whereas the LFC_mid and LFC_high groups showed improvements, but remained below control levels (Fig. 4E). IL-1β levels were reduced by 23.40% in the model group but increased by 7.90% (LF Treat), 12.41% (LFC_low), 4.00% (LFC_mid), and 9.8% (LFC_high) compared with that in the model group. Finally, IL-10 levels were reduced by 22.0% in the model group, with increases of 8.53% (LF Treat), 13.33% (LFC_low), 14.87% (LFC_mid), and 12.05% (LFC_high) after LF intervention (Fig. 4D, F).

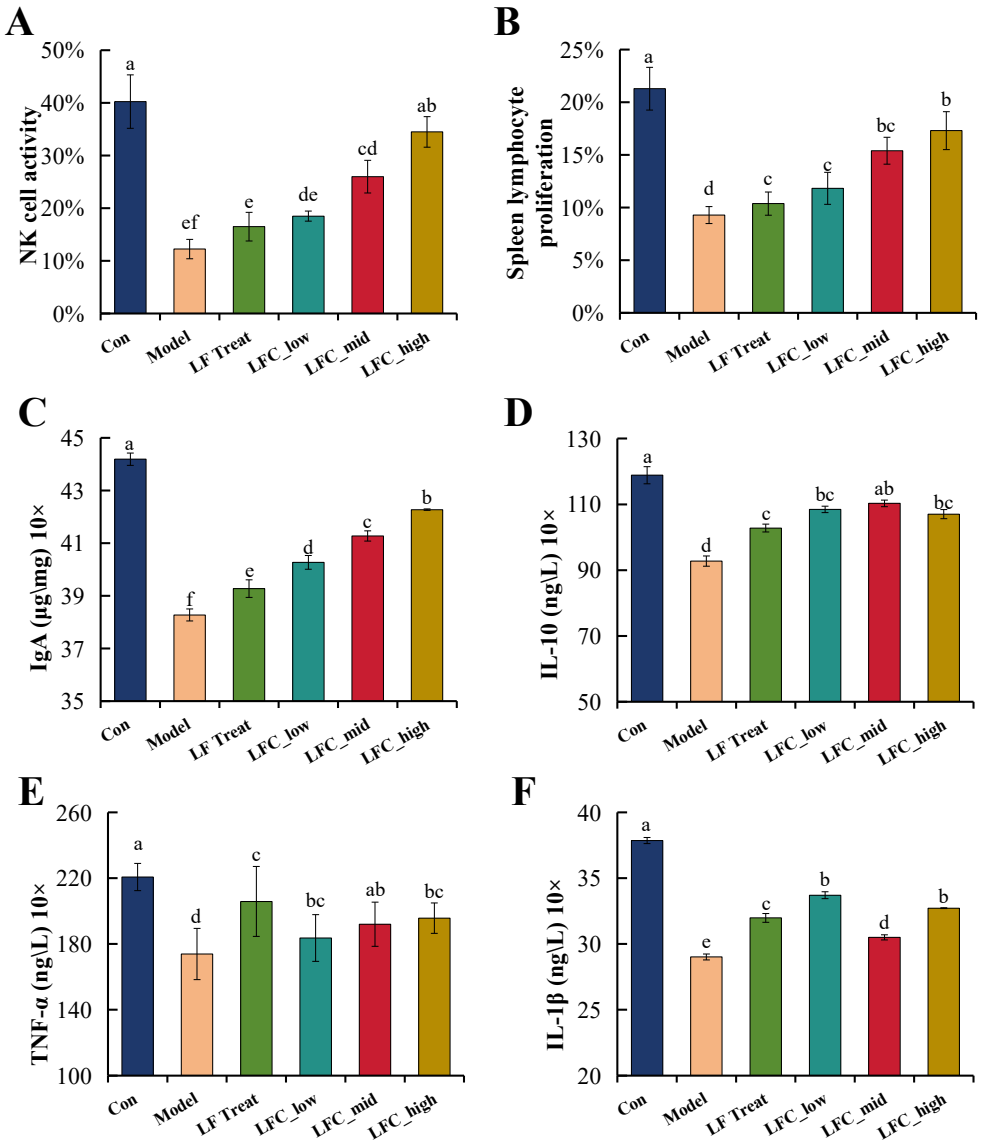

Fig. 4 Effects of the lactoferrin-based formulation on immune cell function and serum cytokine levels in MZD rats. (A) Splenic lymphocyte proliferation capacity assessed by MTT assay upon ConA stimulation. (B) NK cell cytotoxic activity against YAC-1 target cells, measured by lactate dehydrogenase release assay. Levels of (C) IgA, (D) IL-10, (E) TNF-α, and (F) IL-1β were measured by ELISA. Data are presented as mean ± SD (n=4).

3.4 Protective effects of the LF-based formulation on colonic mucosal immunity and barrier morphology in MZD rats

The systemic impact of zinc deficiency on metabolic and mucosal immune markers was evaluated using LDH and sIgA levels[13] (Fig. 5A,B). Compared with the control group, the zinc-deficient Model group exhibited a 12.41% reduction in LDH levels (Fig. 5A), suggesting attenuated cellular metabolism or compensatory stress responses under zinc deprivation. Notably, LF-based formulations restored LDH levels in a dose-dependent manner, with LFC_high achieving near-normal values, indicative of mitigated cellular stress. Concurrently, zinc deficiency significantly suppressed mucosal immunity, as evidenced by a 25.05% decrease in sIgA levels (Fig. 5B). However, LF intervention reversed this deficit, with the high-dose group (LFC_high) restoring sIgA to 120.25 ng/L, exceeding the control levels by 0.33% ($P > 0.05$).

HE and AB-PAS staining of colon sections revealed that prolonged zinc deficiency significantly altered the colonic architecture (Fig. 5C). HE staining showed shallow crypts and reduced mucus layer thickness in zinc-deficient rats, indicating impaired intestinal barrier function and a potential compromise of the intestinal immune system. AB-PAS staining confirmed the reduction in the number of goblet cells. These findings demonstrated substantial zinc deficiency-induced colonic damage, weakening the intestinal barrier and impacting host immunity. However, LF (LF and its formulations) ameliorated these effects, suggesting a protective role in repairing zinc deficiency-induced colonic damage, enhancing intestinal barrier function, and improving immunity. This inverse relationship between LDH and sIgA suggests that LF may protect mucosal immunity by mitigating epithelial cell injury. Elevated LDH levels indicated membrane disruption or cell death, which impairs the microenvironment required for plasma cell-derived sIgA production. In zinc-deficient models, chronic mucosal damage (high LDH levels) often suppressed sIgA secretion by disrupting the crosstalk between intestinal epithelial and immune cells (e.g., plasma and dendritic cells), thereby weakening the mucosal barrier. LF restored both LDH (reduced cell damage) and sIgA (enhanced immune function) levels, implying a coordinated protective effect on mucosal homeostasis.

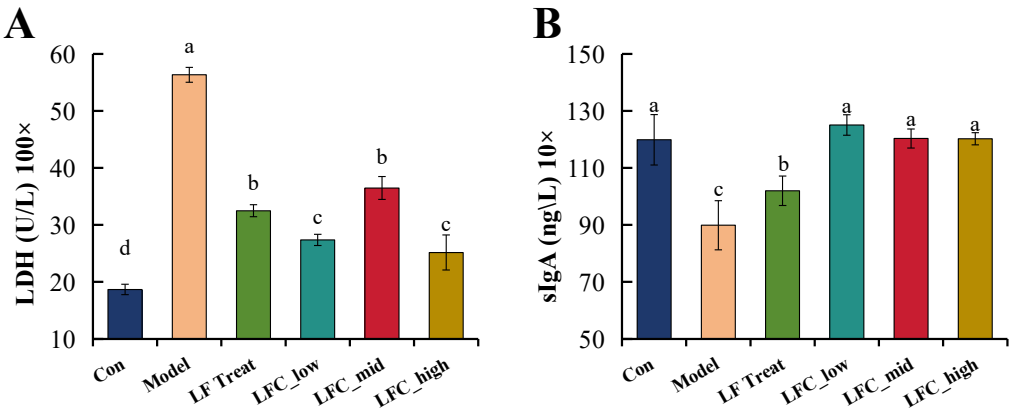

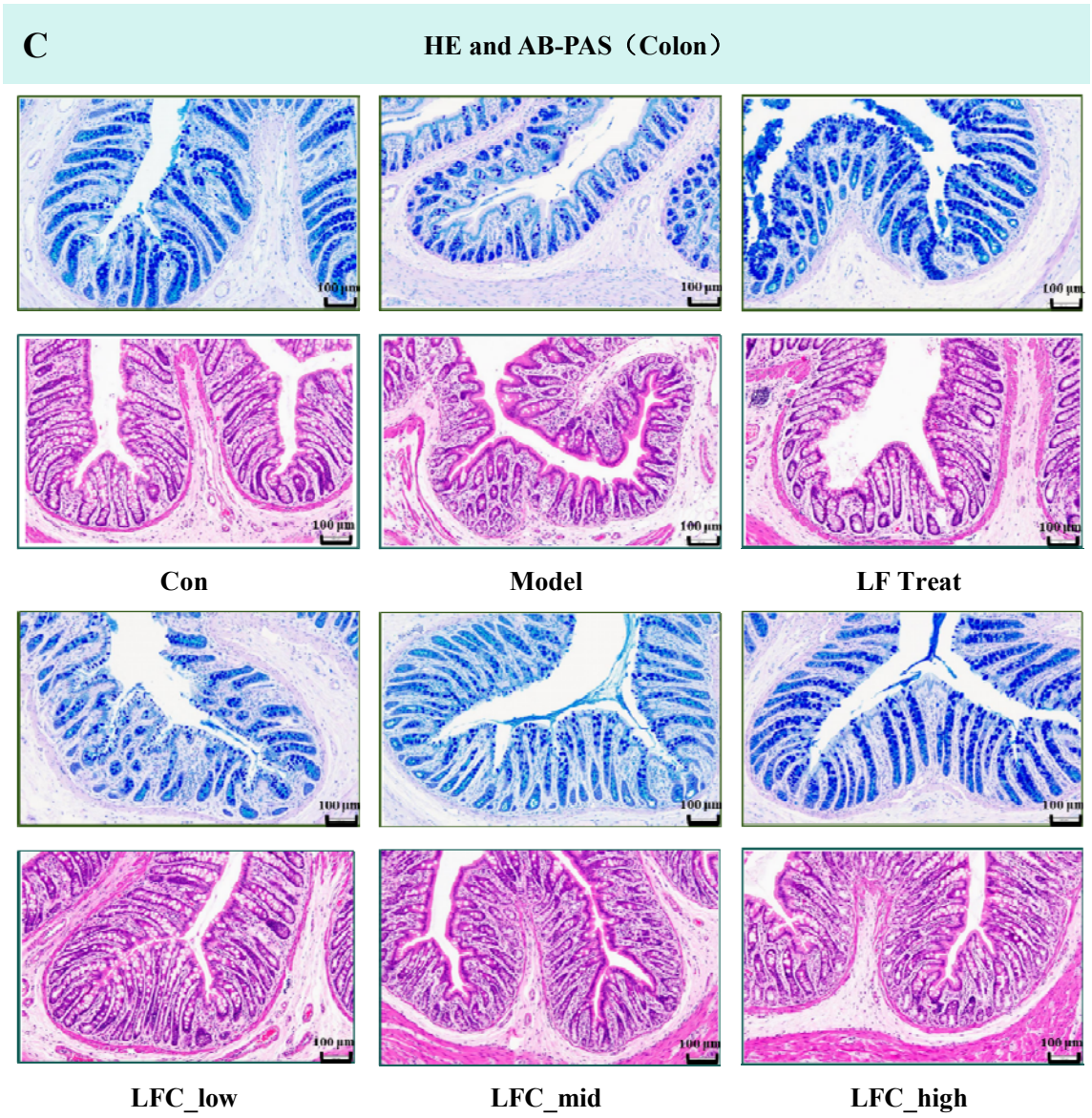

Fig. 5 Assessment of colonic barrier function and mucosal immunity. (A) LDH activity in colon tissue. (B) sIgA levels in colon tissue homogenates. (C) Representative images of colon tissue sections stained with HE and AB-PAS (scale bar = 100 μm). AB-PAS staining highlights goblet cells (magenta) and the mucus layer. Data in A and B are presented as mean ± SD (n=8).

3.5 Modulatory effects of the LF-based formulation on the Th17 and Treg cell regulation in splenic T lymphocytes of MZD rats

Flow cytometry was used to analyze the splenic T lymphocyte subsets, focusing on Th17 and Treg cells (CD3+, CD4+, FoxP3, and IL-17). For Th17 cells (CD4+ and IL-17+), the Model group showed a significantly reduced percentage of Th17 cells (1.13%) compared with that of the control group (2.42%; 57.59% reduction, $P < 0.05$). Intervention with the LF-based formulation alleviated this reduction, with the LFC_high group showing a percentage (2.39%) comparable to that of the control group and significantly higher than that of the other groups. For Treg cells (CD3+ and FoxP3+), the Model group showed a significant reduction (65.93%, $P < 0.05$) compared with that of the control group. Intervention, particularly

with LFC_high (2.40%), increased Treg cell differentiation to levels approaching those of the control group (2.26%, $P > 0.05$) (Fig. 6).

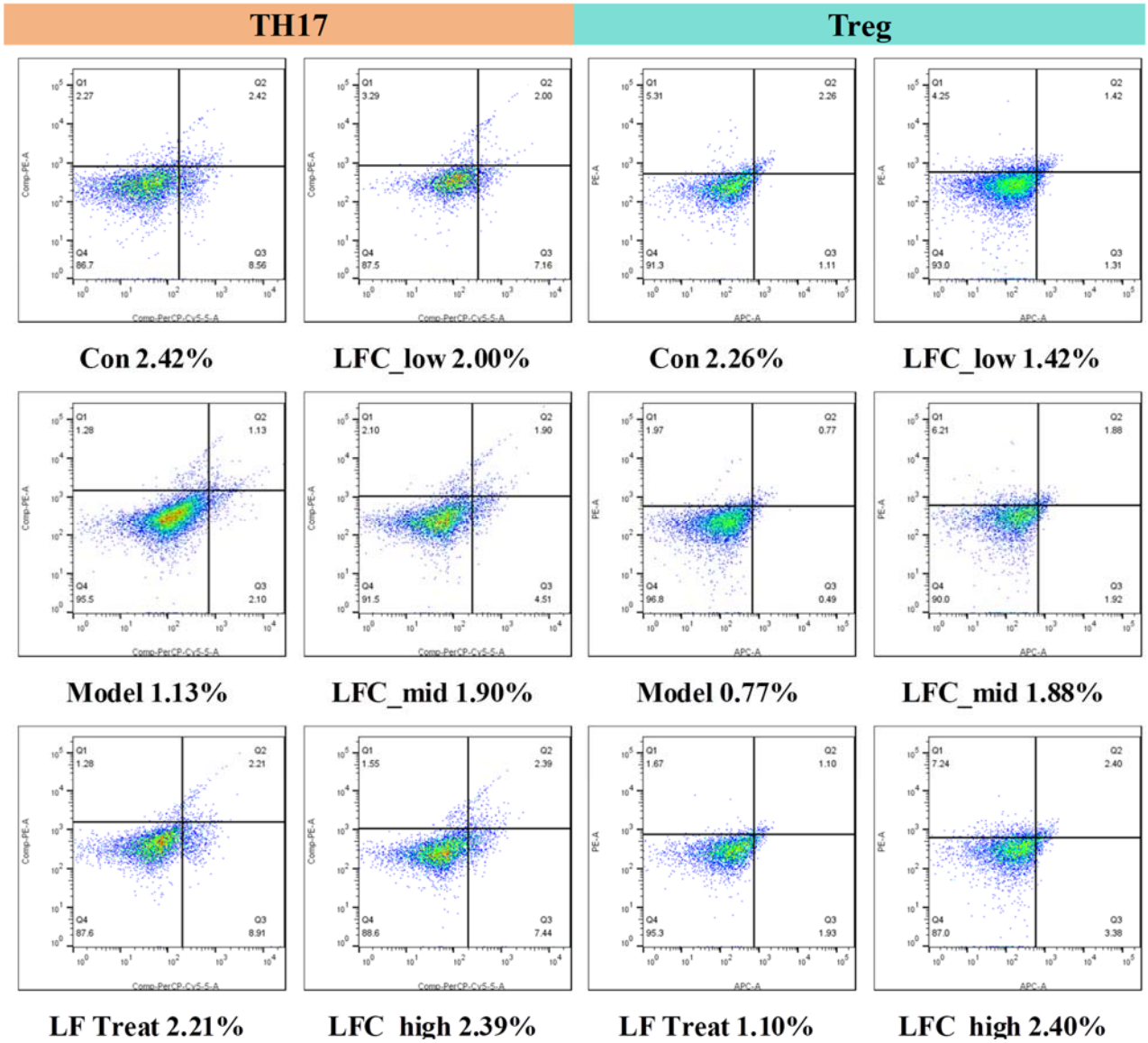

Fig. 6 Modulation of splenic T lymphocyte subsets by the lactoferrin-based formulation

3.6 Correlation analysis of immune-inflammatory biomarkers in MZD rats

This study revealed complex interactions among multiple biomarkers through systematic correlation analysis, providing an important basis for an in-depth understanding of the mechanisms of immune regulation and inflammatory responses. Among the immune-related indicators, the strong positive correlation (r = 0.91) between IgA and IL-10 suggests that they may play a role in immune regulation through a synergistic mechanism. IL-10 enhances mucosal immune responses by promoting B cells to differentiate into plasma cells and secrete IgA[18], which is consistent with the results of the present study. Additionally, the significant correlation between IL-10 and IL-1β (r = 0.83) suggests that the two may be jointly involved in the negative feedback regulation of inflammatory responses through the modulation of the NF-κB or MAPK signaling pathways[19]. Notably, the strong correlation between the splenic index and IgA (r = 0.87) may reflect that the spleen can influence normal IgA production, and interactions between

follicular helper T and B cells in its microenvironment may drive efficient IgA secretion[20]. Among the inflammation-related metrics, the weak positive correlation between TNF-α and LDH (r = 0.46) suggests an association between the inflammatory response and tissue damage. TNF-α causes cellular damage by activating apoptotic signaling pathways (e.g., caspase-3), which releases LDH[21]. However, the weak correlation coefficients suggest that its effects may be influenced by other factors, such as oxidative stress or metabolic abnormalities). Additionally, the very strong positive correlation between NK cell activity and IgA (r = 0.95) may reflect the direct activation of NK cells by IgA via the Fcα receptor (CD89). Some correlations (r < 0.5) between physiological indices (e.g., femur length and weight) and immunoinflammatory indices suggest a correlation between skeletal development and the immune system, with cross-regulation under specific conditions (e.g., chronic inflammatory or metabolic diseases) (Fig. 7).

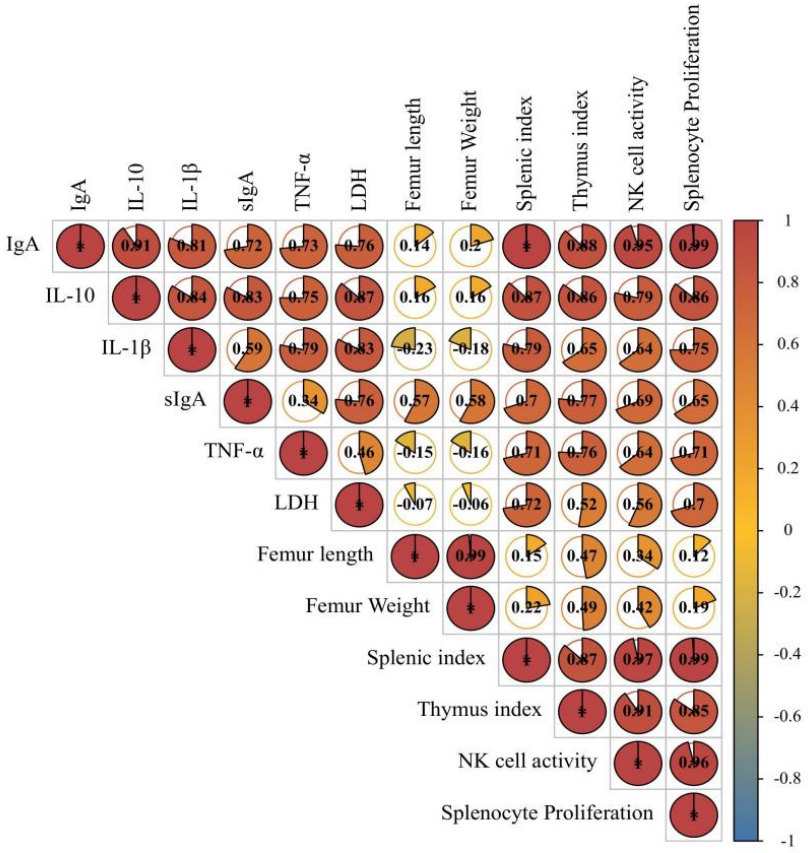

Fig. 7 The correlation analysis of immune and inflammation-related biomarkers. *r = 1

3.7 Regulatory effects of the LF-based formulation on intestinal microbiota composition and diversity in MZD rats

3.7.1 Response characteristics of intestinal microbiota alpha and beta diversity to zinc deficiency and lactoferrin intervention

The *16S* rRNA gene sequencing was used to assess the effect of prolonged zinc deficiency and LF-based interventions on the composition of colonic microbiota. Alpha diversity (Fig. 8A–D), measured using Chao1, species richness, Shannon, and Simpson indices, revealed that Chao1 and species richness were significantly lower in the Model group (P < 0.05) but recovered following the interventions, particularly in the LFC_mid and LFC_high groups, which were not significantly different from those of the

control group ($P > 0.05$). The Shannon and Simpson indices showed similar trends, with significantly higher values in the Model, LF Treat, LFC_low, and LFC_mid groups ($P < 0.05$). The LFC_high group showed increased values, closer to those of the control group, particularly for the Simpson index, indicating higher community diversity.

Beta diversity (Fig. 8E,F), assessed using principal coordinate analysis (PCoA) and non-metric multidimensional scaling (NMDS), revealed that the Model group significantly differed from the control and treatment groups along the PCoA1 and PCoA2 axes ($P < 0.05$), although some similarities were observed along PCoA3. NMDS analysis confirmed that the Model group was significantly different from the control and treatment groups ($P < 0.05$), with the LFC_high group clustering closest to the control group.

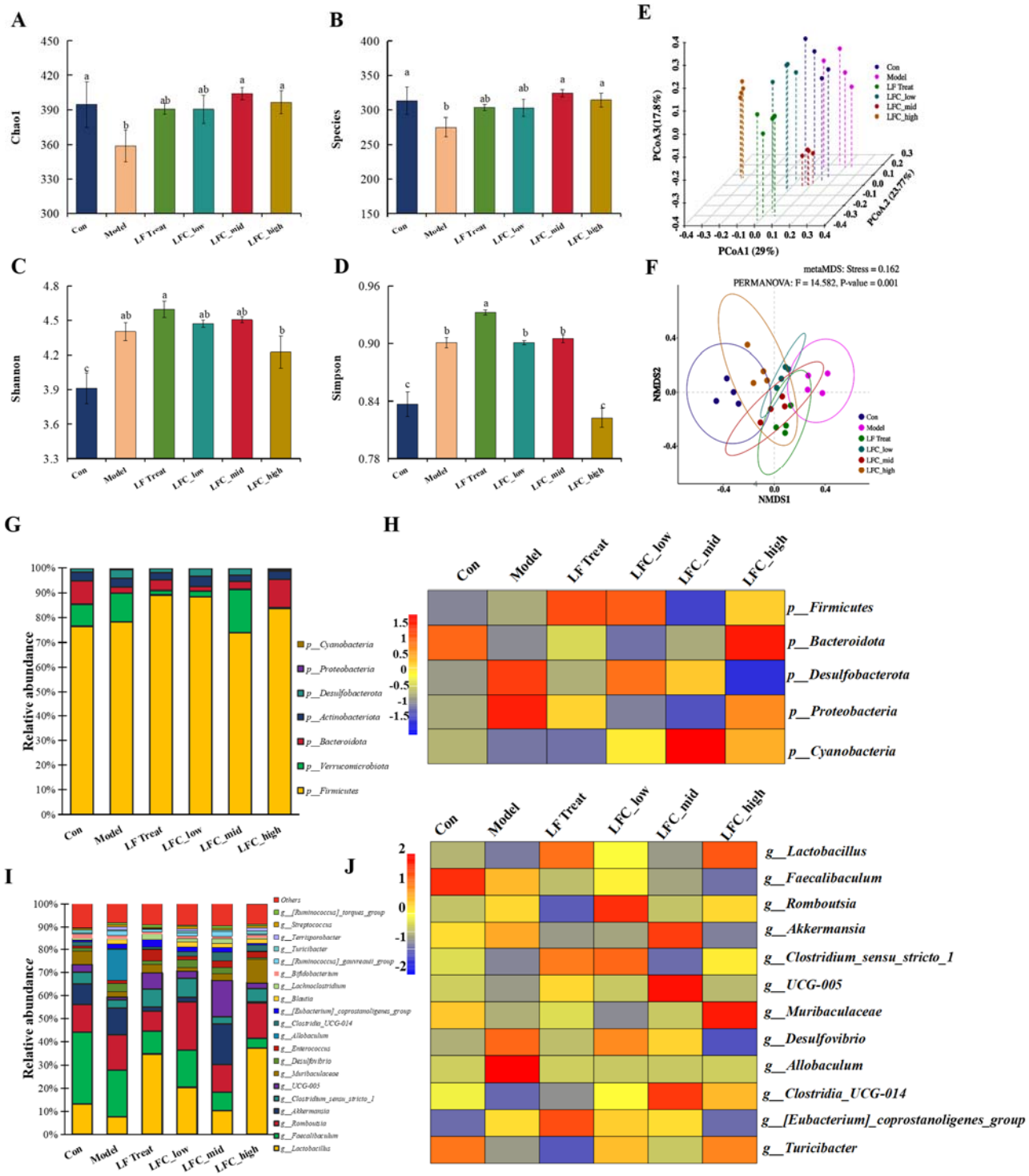

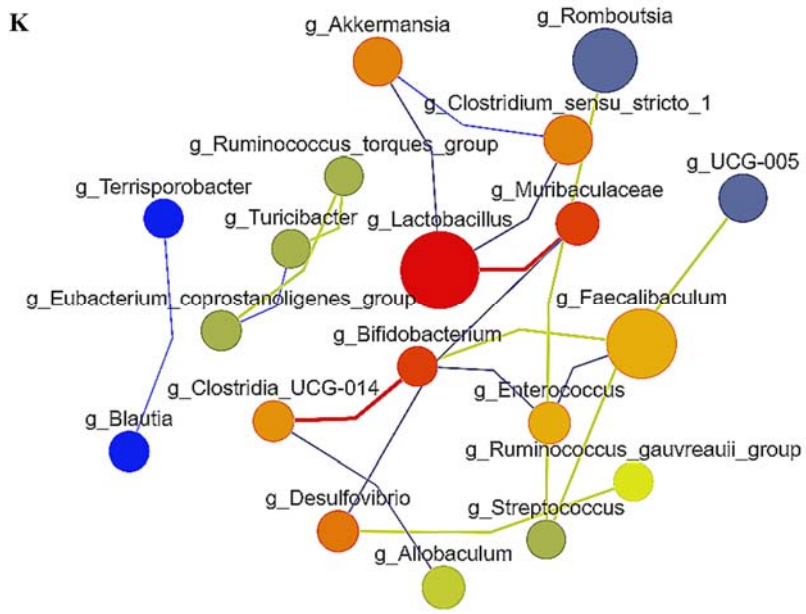

Fig. 8 Different lowercase letters indicate significant group differences (P < 0.05). (A) Chao1, (B)Species richness, (C)Shannon , (D) Simpson, (E) PCoA (Bray-Curtis), (F) NMDS, (G) Phylum-level, (H) Phylum-level heatmap, (I) Genus-level, (J) Genus-level heatmap, (K) Co-occurrence network. Data in A and B are presented as mean ± SD (n=4).

3.7.2 Dynamic changes in the phylum and genus relative abundance and regulation of "core-peripheral" microbial networks in intestinal microbiota

Analysis of the relative microbiota abundance revealed differences across the six groups at both the phylum (7 phyla; Fig. 8G,I) and genus (20 genera; Fig. 8 H,J) levels. The dominant phyla included *p_Firmicutes*, *p_Verrucomicrobiota*, *p_Bacteroidetes*, *p_Actinobacteria*, *p_Desulfobacterota*, *p_Proteobacteria*, and *p_Cyanobacteria*. *p_Firmicutes* predominated the control group but were significantly reduced in the Model group ($P < 0.05$), while *p_Cyanobacteria* and *p_Desulfobacterota* were significantly increased ($P < 0.05$), suggesting gut dysbiosis in zinc-deficient rats. *p_Firmicutes* abundance increased with increasing LF concentration, approaching or exceeding control levels in the LFC_high group, demonstrating the effectiveness of the intervention in restoring the gut microbial balance. *p_Cyanobacteria* abundance decreased with treatment, although it remained slightly higher than that in the control group in the LFC_high group, but significantly lower than that in the Model group ($P < 0.05$). Analysis of the 12 selected genera (Fig. 8J) revealed that *g_Lactobacillus* abundance was higher in the control group but significantly lower in the Model group[22]. The *g_Lactobacillus* abundance initially increased and then decreased with increasing LF concentrations, peaking in the LFC_high group. Conversely, *g_Eubacterium coprostanoligenes* and *g_Clostridia UCG-014* showed opposite trends, with varying responses to treatment. *g_Akkermansia* was significantly higher in the model group than that in the control group, but decreased with treatment. *g_Desulfovibrio* and *g_Enterococcus* also showed varying abundances across groups. The relative abundance of the *g_Ruminococcus gauvreauii group*, *g_Ruminococcus torques group*, and several other genera fluctuated across groups but remained relatively stable overall.

Moreover, we analyzed the role of genus-specific gut microbiota in the multilevel regulation of zinc metabolism (Fig. 8K). The taxa were highly; *g_Enterococcus* and *g_Lactobacillus* significantly influenced zinc bioavailability through zinc-binding proteins (e.g., ZnuABC transporters) and short-chain fatty acid (SCFA) secretion. Specifically, *g_Enterococcus* releases phytate-chelated zinc via phytase activity and indirectly optimizes zinc-mediated T cell function by modulating immune factors, such as IL-10. Additionally, *g_Lactobacillus* enhanced zinc absorption efficiency by upregulating host intestinal zinc transporter (Zip6/ZnT1) expression, and suppressing the proliferation of zinc-dependent pathogens, thereby reducing inflammatory zinc consumption.

Moderately correlated taxa, such as *g_Streptococcu*s, alleviated zinc deficiency-induced oxidative stress through zinc-dependent enzymes (e.g., superoxide dismutase) and synergized with core taxa to maintain intestinal pH balance and promote zinc solubilization. Furthermore, although weakly correlated taxa, such as *g_Akkermansia,* exhibited limited connectivity, their mucin-degrading function was hypothesized to indirectly regulate zinc storage and release within the mucus layer, playing a context-dependent protective role during zinc deficiency-induced intestinal barrier damage. LF restored intestinal zinc homeostasis by chelating zinc to inhibit pathogenic bacterial growth and enabling targeted zinc delivery to host cells, thereby minimizing microbial competition for zinc. These findings indicate that zinc metabolism relies on synergistic interactions between "core-periphery" microbial networks, and LF may provide a precision intervention strategy for zinc deficiency and associated immune-metabolic disorders by modulating the triangular relationship among microbiota, host, and zinc.

4. Discussion

In this study, we investigated the systemic regulatory effects of an LF-based formulation on MZD in rats. LF and its formulations, particularly LFC_high, effectively mitigated growth retardation and immune dysfunction. Femur parameters and immune organ indices were restored to near-control levels [4, 14], and NK cell activity and splenic lymphocyte proliferation confirmed systemic immune reconstitution[15]. Notably, the superior effect of LFC_high over LF alone suggests a synergistic effect between LF, yeast β-glucan, and colostrum[29].

In addition to dose-dependence, the nuanced cytokine profile, such as the targeted inflammatory resolution observed in the LFC_mid group, highlights the sophisticated regulatory capacity of the formulation. To further elucidate these systemic mechanisms, the correlation heatmap analysis (Fig. 9) revealed that MZD disrupted the physiological synergy between growth and immunity. In the MZD model, a robust pro-inflammatory network emerged: TNF-α and IL-1β positively correlated with the cell damage marker LDH, with strong negative correlations with the anti-inflammatory cytokine, IL-10, and mucosal marker, sIgA[30]. This imbalance suggests that MZD-induced sIgA depletion compromised the mucosal integrity and triggered a self-perpetuating inflammatory cycle. Furthermore, the pathogenic *g_Desulfovibrio* was positively linked to inflammation and LDH, whereas the association between beneficial *g_Lactobacillus* and sIgA is weakened, highlighting the link between dysbiosis and mucosal injury[22].

The LF intervention effectively dismantled this pro-inflammatory network and restored systemic homeostasis. The increased abundance of *Lactobacillus* and its strong correlation with sIgA indicates that LF repairs mucosal immunity by modulating the microbiota. *Lactobacillus*-derived SCFAs stimulate pIgR expression to facilitate sIgA secretion, while simultaneously activating GPR43 to suppress NF-κB-mediated pro-inflammatory signaling [23, 24]. Additionally, the iron-binding capacity of LF mitigates oxidative stress, further inhibiting NF-κB[26] and Latif [27], demonstrating the role of LF in enhancing zinc utilization and promoting beneficial microbiota.

Collectively, the LF formulations alleviate MZD through an integrated, multi-pathway network: (1) enhancing zinc bioavailability; (2) directly stimulating systemic immune reconstitution; and (3) reshaping the gut microbiota-immune axis to sustain anti-inflammatory signals[25, 30]. While this animal model provides strong preclinical evidence, future long-term studies are needed to validate these findings in humans[3, 8]. In conclusion, LF-based formulations represent a promising strategy for restoring the biological network synergy between metabolism, immunity, and the microbiome under zinc deficiency conditions.

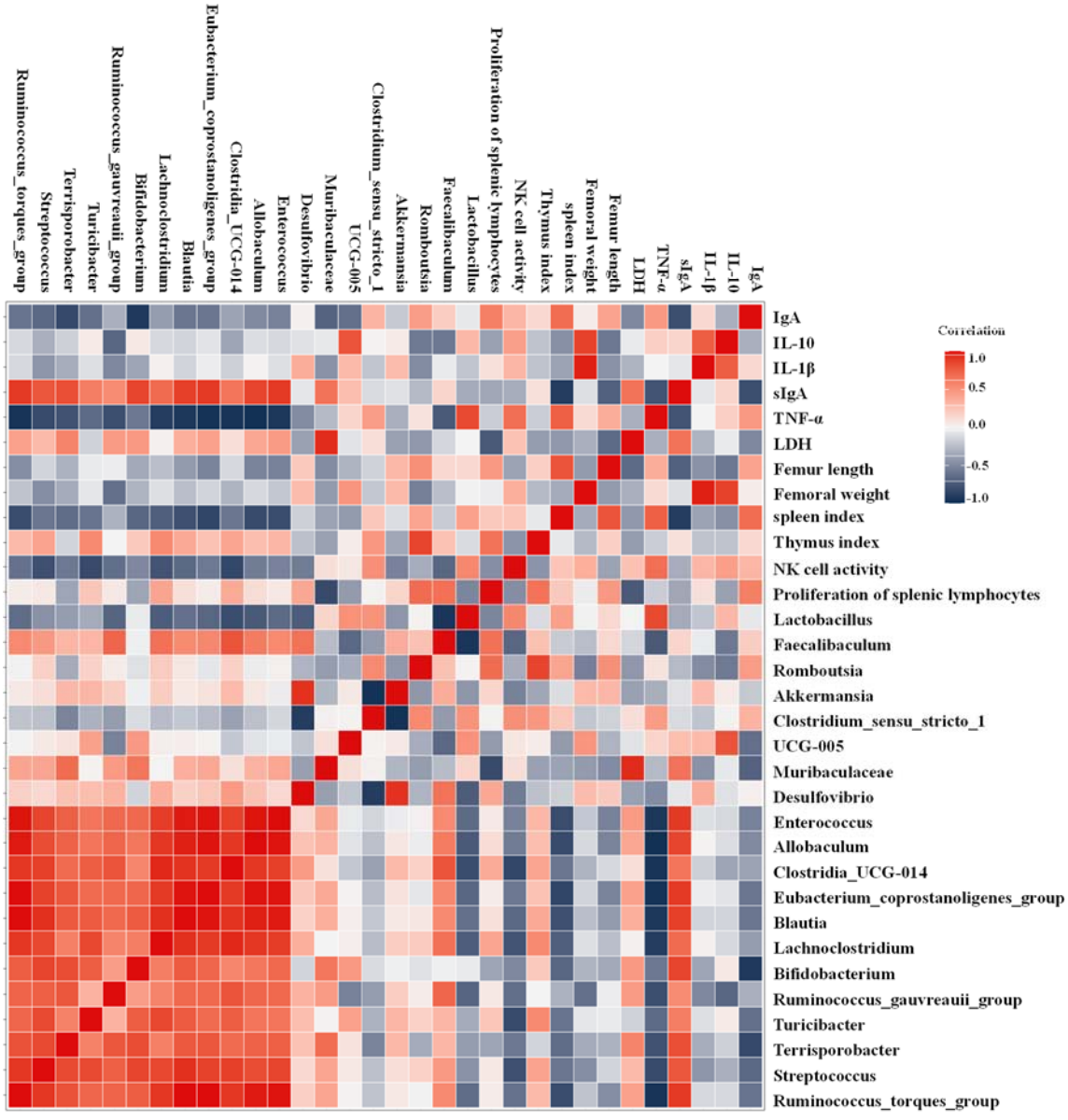

Fig.9 Correlation heatmap of growth parameters, immune indices, and gut microbiota.

5. Conclusion

The LF formulation effectively ameliorated MZD-induced growth retardation, impaired organ development, decreased immune cell function, and abnormal cytokine secretion in rats. LFC_high was particularly effective at promoting femur development, restoring thymus and spleen indices, and enhancing NK cell activity and splenic lymphocyte proliferation. Furthermore, the LF formulation positively modulated the gut microbiota balance, increasing the abundance of beneficial bacteria, such as *g_Lactobacillus,* and decreasing the relative abundance of harmful bacteria, such as *g_Desulfovibrio.* Notably, this study was conducted exclusively in Sprague-Dawley rats, therefore, species differences as well as experimental constraints, limit its generalizability; therefore, the conclusions should not be directly extrapolated to children or human populations. Future studies should focus on broader animal models and more rigorous mechanistic validation, to further clarify the optimal dose and intervention window, and conduct well-designed clinical studies to evaluate the safety, efficacy, and potential applicability in humans.

Conflict of Interest Statement

The authors declare no conflicts of interest.

Fundin

This work were supported by the National Center of Technology Innovation for Dairy (NO.2023-JSGG-9) and the Discovery and Mechanism of Novel Milk-Derived Bioactive Components for Regulating Glucose and Lipid Metabolic Homeostasis(2023YFF1104501-1).

References

[1] Lowe, N. M., Hall, A. G., Broadley, M. R., et al., Preventing and Controlling Zinc Deficiency Across the Life Course: A Call to Action, Adv. Nutr. 15(3) (2024) 100181. https://doi.org/10.1016/j.advnut.2024.100181.

[2] Lu, J., Hu, Y., Li, M., et al., Zinc Nutritional Status and Risk Factors of Elderly in the China Adult Chronic Disease and Nutrition Surveillance 2015, Nutrients 13(9) (2021) 3086. https://doi.org/10.3390/nu13093086.

[3] Magge, H., Sprinz, P., Adams, W. G., et al., Zinc Protoporphyrin and Iron Deficiency Screening, JAMA Pediatr. 167(4) (2013) 361. https://doi.org/10.1001/jamapediatrics.2013.751.

[4] Sun, Y., Chen, J., Wang, H., et al., Correction: Marginal zinc deficiency alters the heart proteome of rats, Food Funct. 14(10) (2023) 4948. https://doi.org/10.1039/d3fo90034g.

[5] Bermejo-Pareja, F., del Ser, T., Valentí, M., et al., Salivary lactoferrin as biomarker for Alzheimer's disease: Brain-immunity interactions, Alzheimers Dement. 16 (8) (2020) 1196-1204. https://doi.org/10.1002/alz.12107.

[6] Hue, D. T., Skirving, R., Chen, T., et al., Colostrum Source and Passive Immunity Transfer in Dairy Bull Calves, J. Dairy Sci. 104 (7) (2021) 8164-8176. https://doi.org/10.3168/jds.2020-19318.

[7] Wang, M., Zhang, L., Yang, R., et al., Improvement of immune responses to influenza vaccine (H5N1) by sulfated yeast beta-glucan, Int. J. Biol. Macromol. 93(Pt A) (2016) 203-207. https://doi.org/10.1016/j.ijbiomac.2016.06.057.

[8] Wang, B., Timilsena, Y. P., Blanch, E., et al., Lactoferrin: Structure, function, denaturation and digestion, Crit. Rev. Food Sci. Nutr. 59(4) (2017) 580-596. https://doi.org/10.1080/10408398.2017.1381583.

[9] Franco, I., Pérez, M. D., Conesa, C., et al., Effect of technological treatments on bovine lactoferrin: An overview, Food Res. Int. 106 (3) (2018) 173-182. https://doi.org/10.1016/j.foodres.2017.12.016.

[10] Rybarczyk, J., Khalenkow, D., Kieckens, E., et al., Lactoferrin translocates to the nucleus of bovine rectal epithelial cells in the presence of Escherichia coli O157:H7, Vet. Res. 50(1) (2019) 75. https://doi.org/10.1186/s13567-019-0694-3.

[11] Yalçıntaş, Y.M., Duman, H., Miranda, J.M., et al., Revealing the Potency of Growth Factors in Bovine Colostrum, Nutrients 16(14) (2024) 2359. https://doi.org/10.3390/nu16142359.

[12] Naiel, S., Dowdall, N., Zhou, Q., et al., Modulating pro-fibrotic macrophages using yeast beta-glucan microparticles prepared by Pressurized Gas eXpanded liquid (PGX) Technology®, Biomaterials 313 (2024) 122816. https://doi.org/10.1016/j.biomaterials.2024.122816.

[13] Mo, X., Sun, Y., Liang, X., et al., Insoluble yeast β-glucan attenuates high-fat diet-induced obesity by regulating gut microbiota and its metabolites, Carbohydr. Polym. 281 (2022a) 119046. https://doi.org/10.1016/j.carbpol.2021.119046.

[14] Li, W., Hu, X., Wang, S., et al., Characterization and anti-tumor bioactivity of astragalus polysaccharides by immunomodulation, Int. J. Biol. Macromol. 145 (2020) 985-997. https://doi.org/10.1016/j.ijbiomac.2019.09.189.

[15] Park, Y. M., Lee, H. Y., Shin, D. Y., et al., Augmentation of NK-cell activity and immunity by combined natural polyphenols and saccharides in vitro and in vivo, Int. J. Biol. Macromol. 268(Pt 2) (2024) 131908. https://doi.org/10.1016/j.ijbiomac.2024.131908.

[16] Wang, H., Zhu, W., Hong, Y., et al., Astragalus polysaccharides attenuate chemotherapy-induced immune injury by modulating gut microbiota and polyunsaturated fatty acid metabolism, Phytomed. 128 (2024) 155492. https://doi.org/10.1016/j.phymed.2024.155492.

[17] Prasad, A.S., Lessons Learned from Experimental Human Model of Zinc Deficiency, J. Immunol. Res. 2020 (2020) 9207279. https://doi.org/10.1155/2020/9207279.

[18] Zhang, B., Vogelzang, A., Miyajima, M., et al., B cell-derived GABA elicits IL-10+ macrophages to limit anti-tumour immunity, Nature. 599(7885) (2021) 471-476. https://doi.org/10.1038/s41586-021-04082-1.

[19] Veenbergen, S., Li, P., Raatgeep, H.C., et al., IL-10 signaling in dendritic cells controls IL-1β-mediated IFNγ secretion by human CD4+ T cells: relevance to inflammatory bowel disease, Mucosal Immunol. 12(5) (2019) 1201-1211. https://doi.org/10.1038/s41385-019-0194-9.

[20] Kanjilal, S., Mina, M. J., Passive immunity for the treatment of influenza: quality not quantity, Lancet Respir. Med. 7(11) (2019) 922-923. https://doi.org/10.1016/s2213-2600(19)30265-6.

[21] van Loo, G., Bertrand, M.J.M., Death by TNF: a road to inflammation, Nat. Rev. Immunol. 23(5) (2022) 289-303. https://doi.org/10.1038/s41577-022-00792-3.

[22] Sauer, A.K., Grabrucker, A.M., Zinc Deficiency During Pregnancy Leads to Altered Microbiome and Elevated Inflammatory Markers in Mice, Front. Neurosci. 13 (2019) 1295. https://doi.org/10.3389/fnins.2019.01295.

[23] Curvelo, J.A.d.R., Barreto, A.L.S., Bayona-Pacheco, B.L., et al., Salivary proteins modulate Candida albicans virulence and may prevent oropharingeal candidiasis, Braz. J. Microbiol. 55 (2024) 3811-3825. https://doi.org/10.1007/s42770-024-01517-5.

[24] Gaulke, C.A., Rolshoven, J., Wong, C.P., et al., Marginal Zinc Deficiency and Environmentally Relevant Concentrations of Arsenic Elicit Combined Effects on the Gut Microbiome, mSphere 3(6) (2018) e00521-18. https://doi.org/10.1128/mSphere.00521-18.

[25] Mayneris-Perxachs, J., Bolick, D.T., Leng, J., et al., Protein- and zinc-deficient diets modulate the murine microbiome and metabolic phenotype, Am. J. Clin. Nutr. 104 (2016) 1253-1262. https://doi.org/10.3945/ajcn.116.131797.

[26] Tian, M., Han, Y., Yang, G., et al., The role of lactoferrin in bone remodeling: evaluation of its potential in targeted delivery and treatment of metabolic bone diseases and orthopedic conditions, Front. Endocrinol. 14 (2023) 1218148. https://doi.org/10.3389/fendo.2023.1218148.

[27] Latif, A., Shehzad, A., Niazi, S., et al., Probiotics: Mechanism of action, Health Benefits and Their Application in Food Industries, Front. Microbiol. 14 (2023) 1216674. https://doi.org/10.3389/fmicb.2023.1216674.

[28] MacManus, C. F., Collins, C. B., Nguyen, T. T., et al., VEN-120, a Recombinant Human Lactoferrin, Promotes a Regulatory T Cell [Treg] Phenotype and Drives Resolution of Inflammation in Distinct Murine Models of Inflammatory Bowel Disease, J. Crohn's Colitis 11(9) (2017) 1101-1112. https://doi.org/10.1093/ecco-jcc/jjx056.

[29] Wong-Chew, R.M., Nguyen, T.V.H., Rogacion, J.M., et al., Potential Complementary Effect of Zinc and Alkalihalobacillus clausii on Gut Health and Immunity: A Narrative Review, Nutrients 16 (2024) 887. https://doi.org/10.3390/nu16060887.

[30] O'Grady, K., Grabrucker, A.M., Metal Dyshomeostasis as a Driver of Gut Pathology in Autism Spectrum Disorders, J. Neurochem. 169 (2025) e70041. https://doi.org/10.1111/jnc.70041.